

PEV Charging Infrastructure Siting Based on Spatial-Temporal Traffic Flow Distribution

Ahmed Abdalrahman, and Weihua Zhuang, *Fellow, IEEE*

Abstract—Plug-in electric vehicles (PEVs) offer a solution to reduce greenhouse gas emissions and decrease fossil fuel consumption. PEV charging infrastructure siting must ensure not only a satisfactory charging service for PEV users, but also a high utilization and profitability for the chosen facility locations. Thus, the various types of charging facilities should be located based on an accurate location estimation of the potential PEV charging demand. In this paper, we propose a spatial-temporal flow capturing location model. This model determines the locations of various types of charging facilities based on the spatial-temporal distribution of traffic flows. We utilize the dynamic traffic assignment model to estimate the time-varying traffic flows on the road transportation network. Then, we cluster the traffic flow dataset into distinct categories using the Gaussian mixture model and site each type of charging facilities to capture a specific traffic pattern. We formulate our siting model as an mixed integer linear programming (MILP) optimization problem. The model is evaluated based on two benchmark transportation networks, and the simulation results demonstrate effectiveness of the proposed model.

Index Terms—Pug-in electric vehicle, charging infrastructure, siting, traffic flow capturing, Gaussian mixture model, integer programming.

I. INTRODUCTION

PLUG-IN electric vehicles (PEVs) are a promising transportation option with many environmental and economic benefits. According to the International Energy Agency (IEA), the number of on-road electrical vehicles is expected to range between 9 million and 20 million by 2020 [1]. To accomplish this ambitious goal, we need overcome some barriers that hinder mass adoption of PEVs. These barriers include PEV cost, negative impacts on the power grid, and availability of charging infrastructure [2].

Various types of charging technologies are available in the market and standardized internationally by the Society-of-Automotive Engineers (SAE). According to SAE J1772 standard, charging levels for PEVs include AC level 1, AC level 2, and DC fast charging [2]. Charging facilities containing AC level 1 or AC level 2 chargers are considered slow since it takes 3-17 hours to charge a PEV battery. Slow charging facilities are commonly located in homes, parking lots in workplaces and shopping centers. Fast charging stations contain DC fast chargers, which can charge a PEV battery up to 80% State-of-Charge (SoC) in approximately 20 minutes. In addition to the plug-in charging facilities, PEVs can be charged without cables through the relatively new wireless power transfer

(WPT) technology [3]. Dynamic wireless charging (or on-road wireless charging) can charge PEVs while they move on roads, which can significantly reduce the onboard battery pack, hence PEVs become lighter in weight and may be less expensive. Currently, several studies and test sites are underway to develop the dynamic chargers [4]. For example, the fifth-generation of the on-line electric vehicles (OLEVs) project, led by KAIST, can obtain WPT with 22 kW maximum pick-up power and maximum efficiency 91% at 9.5 kW with 20 cm air gap [5].

PEV charging infrastructure siting is a problem of strategically locating various types of charging facilities in a network, while considering unique characteristics and usage patterns of each facility type. The siting problem is technically challenging since PEVs are characterized by their limited driving range, in addition to the randomness in driving patterns and charging decisions of PEV users. Furthermore, each type of charging facility must be sited in locations that conform to the requirements of the PEV users in order to maximize their satisfaction. Due to the high capital cost associated with charging facility construction, the planning body must ensure high utilization and profitability of the chosen facility locations [6]. Charging facility utilization will be maximized if they are close to demand locations. However, PEV charging demand is closely related to driving behavior, which varies from one customer to another. Thus, charging infrastructure siting should be based on an accurate location estimation of the potential PEV charging demand [7].

There are two basic categories of charging facility siting models based on demand estimation methods: nodal PEV density-based models and traffic flow-based models [2]. In the traffic flow-based models, PEV users are assumed to prefer charging their vehicles during trips to destination locations [8]. Thereby, the traffic flow conditions on the road system can be used to estimate potential PEV charging demand. When the traffic volume on a particular road is high, there is a high probability that the charging demand on that road will be high, and vice versa [9]. Traffic flow is defined as the number of vehicles which travel along the links that connect different transportation network nodes from an origin to a destination along a pre-determined travel route [8]. Flow capturing models are used to locate the charging facilities on the traveling routes to maximize the captured traffic flows. Note that the traffic flows are origin-destination (OD) flows, not link flows. Although link flows are easier to obtain from vehicles count data than OD flows, flow capturing models utilize OD flows in locating the facilities [10]. This is because flow capturing models prevent flow double counting, which is the capture of

The authors are with the Department of Electrical and Computer Engineering, University of Waterloo, Waterloo, ON, Canada. (e-mail: aabdalra@uwaterloo.ca; wzhuang@uwaterloo.ca).

a flow more than once at the expenses of other flows in the network that have not been captured at all. When link flows are used in these models, traffic flows that passes over many links can be captured more than once.

Several flow capturing models are proposed in the literature to site a single type of the charging facilities [11]. Flow-capturing location model (FCLM) is one of the early models, which sites charging facilities to maximize the captured passing flows. Traffic flow is considered captured if there is a charging facility located on the flow path [12]. An extended version of FCLM has been developed to consider the limited driving range of PEVs [10] [13], which allows PEV users to have long-distance trips via multi-stop charging. The FCLM is further developed to minimize the number of required charging facilities by considering the deviation paths under an assumption that PEV users may accept slightly longer trips to charge their vehicles [14] [15]. Additionally, the uncertainty of the traffic flows can be addressed to account for the future adoption of PEV charging demand [16] [17].

Existing flow capturing models are based only on the spatial distribution of traffic flows under the assumption that drivers always choose the route with the shortest driving distance between any OD pair. This assumption simplifies the estimation of driver route choices. However, traffic flows can be over-estimated for some roads if driver route choices are governed only by the distance between OD pair. Moreover, the assumption neglects the impact of time-dependent dynamics of traffic flows. In reality, drivers use various routes between the same OD pair to avoid traffic congestion. Temporal traffic distribution contributes to accurately estimating the spatial traffic distribution. Some traffic phenomena, such as road congestion, dynamic routing and peak spreading, can only be described using the temporal dimensions of traffic flows. It is more practical that drivers choose the routes with minimum travel times to their destinations, considering various user departure times and network congestion. Thus, both the spatial and temporal distributions of traffic flows should be used in estimating the PEV charging demand.

Deployment of multiple types of charging facilities is studied in [18] [19], which adopt the tour-based approach in siting multiple types of charging facilities. In this approach, PEVs are assumed to travel through a tour of several sequential series of destinations, and the dwelling time at each destination is known. Then, the siting model deploys suitable types of charging facilities at destination nodes to utilize the dwelling time of the users. It is assumed that the trajectory and usage patterns of all PEVs in the system are known. This information may not be available in a system with a large fleet of PEVs.

The economic aspects in the placement of multiple-types of charging technologies are studied in [20] [21] [22]. The objectives of these studies are to minimize either the personal charging cost or the social cost of the charging infrastructure. From the perspective of the system planner, integrated planning frameworks with multiple-types of charging facilities are presented in [20] [22]. In [20], each charging service provider offers a charging service with a particular charging technology. The service providers compete with each other in choosing service locations and prices. The social cost of the entire

TABLE I
SUMMARY OF PEV CHARGING INFRASTRUCTURE SITING MODELS

Function	Study	Main feature
Siting a single type of facilities	[12]	Maximize the captured traffic flows
	[10] [13]	Consider the limited PEV driving range
	[14] [15]	Consider the deviation paths of drivers
	[16] [17]	Consider the uncertainty of traffic flows
Siting multiple types of facilities	[18] [19]	Consider the multiple charging rates of charging facilities
	[20] [22]	Minimize the social cost of charging infrastructure
	[21]	Minimize the charging cost of PEVs

charging infrastructure can be minimized by considering the substitution effect among different types of charging facilities [22]. From the perspective of PEV users, an agent-based model can be used to characterize the interaction between PEV drivers and charging infrastructure. Multiple-types of charging facilities can then be sited in locations that minimize the charging cost of each PEV, including the opportunity cost of driver's time [21]. This approach is important in the high-level planning context; however, it does not account for the traffic conditions and congestion in identifying areas where it is more likely to use a certain type of charging facilities.

A summary of main features of the charging infrastructure siting approaches is given in Table I. A more comprehensive survey can be found in [2] [11]. In this paper, we investigate and develop a spatial-temporal flow capturing location model (ST-FCLM) for siting various types of PEV charging facilities on the transportation network. The ST-FCLM accounts not only the transportation network dynamics and congestion, but also the different characteristics and usage patterns of each charging facility type. The major contributions of this study are as follows:

- First, our model extends the existing flow capturing models by addressing the dynamic traffic flows rather than static flows. We consider all the feasible routes that travelers may choose for each OD pair to minimize their travel time in this formulation. Moreover, travelers' departure times and congestion levels on the road network are inherently accounted in the time-varying traffic flows, which we extract from a simulation-based dynamic traffic assignment (DTA) model;
- Second, our model locates multiple types of charging facilities, taking advantage of the unique characteristics and usage patterns of each charging technology. Towards this end, we partition the traffic flow dataset into distinct categories by using the Gaussian mixture model-based clustering (GMM). Then, we site each type of charging facility to capture a specific traffic pattern.

The remainder of the paper is organized as follows. The system model is presented in Section II, along with a discussion on the dynamic traffic assignment model. In Section III, we discuss how to cluster the traffic flow dataset using the Gaussian mixture model, and formulate the ST-FCLM as an optimization problem. Section IV presents the sizing of charging facilities based on queuing theory. Numerical

results are given in Section V to evaluate the proposed model. Finally, Section VI draws some conclusions from this study and presents a possible future extension for our model.

II. SYSTEM MODEL

Consider a typical metropolitan area with road transportation network $T_N(N_T, L_T)$, where N_T is a finite set of nodes and L_T is a finite set of directed links connecting the network nodes. Transportation system nodes can represent road intersections, highway exits, or locations with high traffic. The links represent streets, roads, traffic lanes, etc. Vehicles are assumed to start daily trips from a set of origins represented by \mathcal{O} ($\mathcal{O} \subseteq N_T$) to a set of destinations represented by \mathcal{D} ($\mathcal{D} \subseteq N_T$). Traffic demand at the origin nodes is considered to be deterministic and independent of the traffic conditions in the network. Let a ($a \in L_T$) denotes a link, and r a route. A list of connected links $\{a_1, a_2, \dots, a_m\}$ connect origin o ($o \in \mathcal{O}$) and destination d ($d \in \mathcal{D}$). In order to represent each OD pair, the single subscript q is replaced the double subscript od . Let R_q denote the set of all feasible routes that a driver may choose to travel between an OD pair q . Let $f_{q,r}(t)$ represents the time-varying traffic flow (i.e., vehicles volume per unit time) over the route r ($r \in R_q$) between OD pair q at time t . Time is partitioned to discrete time periods, $t = 0, \dots, T$, where T is the end of assignment horizon and the network is assumed empty at $t = 0$. Individual drivers are assumed seeking routes that minimize their traveling times, which is known as user equilibrium.

A. PEV Charging Infrastructure

There are three types of public charging facilities available in the system: parking lots with slow chargers (PLs), fast charging stations (FCSs), and on-road wireless chargers (OWCs). PEV users can choose any of these technologies to charge their PEV batteries. Each PEV in the system starts its daily trips with at least half full battery charge. A PEV can be charged by plugging a cable into a charger in a PL or an FCS. The charging time in PLs is relatively longer than that with FCSs. Thereby, PLs are deployed on the destination nodes of the daily trips, such as workplaces and shopping centers. FCSs are deployed on the transportation system nodes, such as road intersections. Additionally, some PEVs in the system capable of charging through wireless power transfer technology in OWCs, which are deployed on the surface of dedicated road lanes, represented by transportation system links.

B. Dynamic Traffic Assignment

The dynamic traffic assignment model forecasts traffic load in time-varying traffic patterns among transportation system roads [23]. Different from the static traffic estimation models, the DTA model describes effects such as network congestion and queuing, due to vehicles accumulation on the transportation network links if link inflows exceed link outflows [24] [25]. In DTA, travelers are assumed to choose routes that minimize their experienced travel time between an OD pair, considering congestion levels in the whole network [26]. Travelers then choose time-dependent shortest routes instead of the

shortest distance route, which are likely to differ significantly. Since link travel times change dynamically, depending on the time departure from the route origin and the traffic conditions encountered along the route. The traffic flows on roads at a particular time are then affected by the flows that may depart previously as well as the flows that will depart subsequently. The traffic flow history on the network has a direct impact on the traffic flows on roads [23]. To approximate traveler route choices, Wardrops user-equilibrium principle is used. This principle states that the routes used by all travelers between the same OD pair at the same departure time have equal and lowest experienced travel time, and no user can lower his experienced travel time through unilateral actions [23]. Thereby, the DTA model excludes impractical routes such as routes including loops or routes with a high traveling time. In simulation-based DTA, time-varying flows that satisfy the dynamic user equilibrium are determined through iterative procedures [23].

The DTA model requires time-dependent OD matrices, which specify individuals' traveling demands. OD matrices are generated by dividing the given area into zones. Then, the number of trips that begin or end in each zone, as well as when these trips will occur, are aggregated. Most urban planning and transportation agencies have OD matrices extracted from travel surveys conducted every 5-10 years [23]. These surveys contain information about trips made by individuals on a typical weekday such as origin, destination, start time, purpose, etc. OD matrices can also be estimated via other techniques such as mobile phone data [27]. Usually, OD matrices change slowly over a long time period, influenced by human factors such as socio-economic and environmental status [28].

III. SPATIAL-TEMPORAL FLOW CAPTURING LOCATION MODEL

PEV charging infrastructure siting is a problem of strategically locating various types of charging facilities in a network. The ST-FCLM presented in the following is to site a given number of charging facilities in locations that maximize the captured traffic flows. PEV charging infrastructure contains three types of facilities, including OWCs, FCSs, and PLs. These facilities are to meet varying demands or preferences of PEV users, which can be either *en route* during the traveling from origins to destinations or *static* at the trip destinations. Practically, a PEV driver tends to charge a PEV at the trip destination if the PEV has enough SoC to complete the trip and there is a charging facility at the destination, to avoid waiting time at charging facilities. On the other hand, *en route* PEV charging will be limited to the situations where the SoC of PEV battery falls below a certain threshold or for a long distance trip [29]. Planning of PEV charging infrastructure should satisfy both types of charging demand (*en route* and *static*) to meet critical service requirements.

Both OWCs and FCSs are suitable for meeting the *en route* charging demand, as users in general would prefer spending less time in charging facilities during the trips. The traffic flows during peak traffic periods are captured by the OWCs. The chosen OWC locations should intercept the maximum amount

of traffic flow during the peak traffic periods. These locations are likely to be congested, which is more appropriate for the usage of OWCs. This is because vehicles speed will be lower and PEVs will be on top of the charging lanes for a longer time, thus allowing PEVs batteries to be charged by a larger amount of energy. Additionally, during the peak traffic hours, drivers will be highly motivated to use OWCs to charge their PEVs while driving, instead of waiting for charging service at a plug-in charging facility. The traffic flows during non-peak traffic periods are captured by the FCSs, since a PEV user is more likely to stay for some time at FCS for battery charging, including the battery charging time and the waiting time for charging service.

In addition to the *en route* PEV charging demand, users may need to charge their PEVs at trip destinations. This type of charging demand is considered *static*, as users utilize their dwelling time at destination nodes, in which PEVs are parked for several hours, such as working hours or overnight parking. The *static* PEV charging demand can be captured by PLs at the destination nodes of traffic flows. In this way, *en route* PEV charging demand will be covered during traveling between OD pairs by either OWCs or FCSs, and during parking at destination nodes by PLs. Consequently, the unique characteristics and usage patterns of the three types of charging facilities are considered in our proposed siting model.

To develop the ST-FCLM, we make some assumptions: 1) Drivers always choose the route that minimizes their personal travel time between each OD pair, considering departure time and congestion levels in the transportation network; 2) PEVs are assumed to be uniformly distributed across the given area and the PEV penetration rate is known. Currently, this assumption may not be accurate in many cities because PEV users have a certain income level and reside in some city regions. Our model and analysis can be extended to account for a non-uniform PEV distribution, provided such a distribution is available; 3) PEV driving range and energy consumption per unit distance are similar in all PEVs in the system, equal to the average of various PEV classes.

Our approach for developing the ST-FCLM is comprised of the following steps: 1) To estimate the spatial-temporal traffic flows within the given study area using a simulation based DTA model; 2) To distinguish between siting locations of various charging facility types. To accomplish this task, the traffic flow dataset is clustered according to the temporal characteristics based on the GMM algorithm. Then, we site each type of charging facilities to capture a distinct traffic pattern; 3) To generate a set of candidate sites in order to consider the PEV limited driving range. Hence, more than one charging facility may be allocated between an OD pair in the network if the traveling distance between them is longer than the maximum PEV driving range.

A. Clustering The Traffic Flow Dataset

Recall that the exogenously generated traffic flow dataset, $\mathcal{F} = \{f_{q,r}(t)\}, \forall q, r, t$, represents the traffic volume on route $r \in R_q$ between OD pairs $q \in Q$ at time slot $t \in T$ of a typical weekday. Thus, $\mathcal{F} \in \mathbb{R}^{\mathcal{N}, T}$ is a matrix, where

\mathcal{N} denotes the number of flow vectors and T denotes the time periods. Each flow vector $f_{q,r} = [f_{q,r}^1, f_{q,r}^2, \dots, f_{q,r}^T]$ represents the discretized time-varying flow volumes between on corresponding route and between the corresponding OD pair. For \mathcal{N} flow vectors in the transportation network, the traffic flow dataset is denoted as follows:

$$\mathcal{F} = \begin{bmatrix} f_{1,1}^1 & f_{1,1}^2 & f_{1,1}^3 & \dots & f_{1,1}^T \\ \vdots & \vdots & \vdots & \ddots & \vdots \\ f_{q,r}^1 & f_{q,r}^2 & f_{q,r}^3 & \dots & f_{q,r}^T \\ \vdots & \vdots & \vdots & \ddots & \vdots \\ f_{Q,R_q}^1 & f_{Q,R_q}^2 & f_{Q,R_q}^3 & \dots & f_{Q,R_q}^T \end{bmatrix}.$$

In order to site each type of charging facilities in locations that capture distinct traffic patterns, the time-varying traffic flows are clustered according to their similarities.

Definition 1. The clustering process is to partition \mathcal{F} into k clusters $\{\theta^1, \theta^2, \dots, \theta^k\}$ according to a similarity measure, where each cluster $\theta^i \subseteq \mathcal{F}$, ($i = 1, 2, \dots, k$) has a common characteristic.

Traffic flow dataset is clustered according to the temporal characteristics. The goal of clustering is to categorize the time periods in which the traffic flows are either high or low. More precisely, the clustering objective is to develop two heat maps that reflect the relative need for each type of charging facilities: 1) The first heat map is for the aggregated traffic flow during the peak traffic period, which is used to site OWCs; 2) The second heat map is for the aggregated traffic flow during the non-peak traffic period, which is used in siting FCSs. Additionally, PEV numbers are aggregated over time at the destination nodes to reflect the relative need for PLs at these nodes. All types of charging facilities in the system can be used by PEV users at anytime of day and those heat maps are only used for selecting appropriate locations for each charging facility type. Towards this end, the Gaussian mixture model-based clustering can be used, which is characterized by its speed of convergence and adaptability to sparse data [30]. Another key feature of the GMM algorithm is its soft assignments of data points to clusters. In the soft assignment, data points can be assigned to multiple clusters with certain probabilities [30]. The soft assignment feature facilitates accurate clustering of the traffic flow dataset.

The GMM is a probabilistic model that assumes all data points are generated by a mixture of a finite number of Gaussian distributions, in which each Gaussian component represents a unique cluster [31]. To cluster the traffic flow dataset according to the temporal characteristic, the spatial dimension of the data is ignored, and temporal distance function is used to determine the dissimilarity between clusters. The traffic flow dataset is then represented as $\mathcal{F} = \{f_1, \dots, f_T\}$, and the t th entry of a T -dimensional discrete-valued data vectors represents a vector of traffic flows via all routes and OD pairs on time t . For the GMM with k components, the density of f_t is a sum of weighted Gaussian densities $\{\theta(\mu_i, \Sigma_i)\}_{i=1}^k$ as given by the following equation [31] [30]:

$$p(f_t | \lambda) = \sum_{i=1}^k \omega_i \theta(f_t | \mu_i, \Sigma_i) \quad (1a)$$

$$= \sum_{i=1}^k \omega_i \frac{\exp(-\frac{1}{2} (f_t - \mu_i)^\top \Sigma_i^{-1} (f_t - \mu_i))}{(2\pi)^{T/2} |\Sigma_i|^{1/2}} \quad (1b)$$

where ω_i represents the weight of the i th Gaussian component with $\sum_{i=1}^k \omega_i = 1$. The mean vector and the covariance matrix are denoted by μ_i and Σ_i , respectively. The complete GMM parameters are represented by the mean vectors, covariance matrices and mixture weights of all the Gaussian component densities. These parameters are collectively denoted by $\lambda = \{\omega_i, \mu_i, \Sigma_i\}, i = 1, \dots, k$.

Ideally, one should use the maximum likelihood (ML) estimation method in order to estimate the GMM parameters that best fit the distribution of the data vector. By assuming the independence among the data points, the log-likelihood function (\mathcal{L}) is given by the following equation [31]:

$$\mathcal{L} = \ln p(\mathcal{F} | \lambda) = \sum_{t=1}^T \ln \left\{ \sum_{i=1}^k \omega_i \theta(f_t | \mu_i, \Sigma_i) \right\}. \quad (2)$$

However, this equation is a nonlinear function of λ , making it difficult to maximize its expression [31] [30]. Instead, the expectation-maximization (EM) algorithm can be used to estimate the GMM parameters. The EM algorithm performs two iterative steps, which are the expectation step (\mathbb{E} -step) and the maximization step (\mathbb{M} -step) [31] [30]. The algorithm starts with the \mathbb{E} -step by picking an initial guess about the GMM parameters, then computes the posterior probabilities (or membership probabilities) of the given data, which maximize the expected log-likelihood function. Using the current GMM parameters values, the posterior probability of data item t belongs to component j is denoted by (p_{tj}) , and is given by

$$p_{tj} = \frac{\omega_j \theta(f_t | \mu_j, \Sigma_j)}{\sum_{i=1}^k \omega_i \theta(f_t | \mu_i, \Sigma_i)}. \quad (3)$$

Afterwards, the \mathbb{M} -step updates the GMM parameters based on the current posterior probabilities, as given by

$$\omega_j^{new} = \frac{1}{T} \sum_{t=1}^T p_{tj}, \quad j = 1, \dots, k \quad (4a)$$

$$\mu_j^{new} = \frac{1}{T \omega_j^{new}} \sum_{t=1}^T p_{tj} f_t, \quad j = 1, \dots, k \quad (4b)$$

$$\Sigma_j^{new} = \frac{1}{T \omega_j^{new}} \sum_{t=1}^T p_{tj} (f_t - \mu_j^{new})(f_t - \mu_j^{new})^\top, \quad (4c)$$

$$j = 1, \dots, k.$$

The EM algorithm converges when the changes in the log-likelihood function or alternatively in the GMM parameters are less than a given threshold value (δ). The termination condition of the EM algorithm is when $|\mathcal{L}^{new} - \mathcal{L}| < \delta$. Thus, the EM algorithm evaluates the log-likelihood function, as given by Equation (2).

The number of components in GMM can be efficiently selected based on the Bayesian information criterion (BIC) [30] [32]. The basic idea of the BIC is that adding more components or clusters to the GMM will increase the value of the likelihood function, although the complexity of the

model will increase as the GMM parameters increase. The BIC resolves this issue by penalizing the GMM complexity by the addition of more components. The formula of the BIC is given by

$$BIC = -2\mathcal{L} + k \ln T \quad (5)$$

where \mathcal{L} is the maximized value of the likelihood function; k denotes the number of components or clusters in the GMM; T denotes the number of data points in the clustered dataset. The optimal number of components of the GMM is k^* that minimizes the BIC score, as given by the following equation:

$$k^* = \arg \min_{k \in \mathbb{N}} BIC. \quad (6)$$

B. Optimization Problem

Based on the clustered traffic flow dataset, the GMM computes the membership probability for each time slot to the corresponding output label. The cluster that is parameterized with the highest mean value is labeled as the peak traffic flow cluster. Vector $\mathbb{P}^R = [p_1^R \ p_2^R \ \dots \ p_T^R]^\top$ contains the membership probability for data points with respect to the peak traffic flow cluster. Each element in that vector, p_t^R , represents the probability of the observed flows at time slot t belongs to the peak traffic flow cluster.

The ST-FCLM model captures the cumulative traffic flows over peak traffic periods by the OWCs, and the cumulative traffic flows over non-peak traffic periods by the FCSs. The cumulative traffic flows during the peak ($\Phi^R \in \mathbb{R}^N$) and non-peak ($\Phi^N \in \mathbb{R}^N$) traffic periods are defined as

$$\Phi^R = \mathcal{F} \cdot \mathbb{P}^R = \sum_{t=1}^T f_{q,r}(t) p_t^R \quad \forall q \in Q, r \in R_q \quad (7a)$$

$$\Phi^N = \mathcal{F} \cdot \mathbb{P}^N = \sum_{t=1}^T f_{q,r}(t) p_t^N \quad \forall q \in Q, r \in R_q \quad (7b)$$

where \mathbb{P}^N is a vector that contains the membership probability for data points with respect to the non-peak traffic flow cluster. If the GMM partitions the traffic flow dataset with more than two components, we can then set $\mathbb{P}^N = 1 - \mathbb{P}^R$. The probability vectors act as weights to the traffic flow dataset that facilitates the evaluation of the cumulative traffic volumes on roads during various time windows.

The static charging demand of PEVs at the trip destinations can be reflected by the number of PEVs at destination nodes. The PEVs static charging demand can be estimated based on the cumulative traffic flows over time via all routes between each OD pair q . Hence, PEVs static charging demand ($\Phi^S \in \mathbb{R}^Q$) is defined as

$$\Phi^S = \sum_{t \in T} \sum_{r \in R_q} f_{q,r}(t) \quad \forall q \in Q. \quad (8)$$

The objective of the ST-FCLM is to choose the best locations, which maximize the captured traffic flows, for each type

of charging facilities. The ST-FCLM is formulated as follows:

$$\max_{\mathbf{X}} \left\{ \sum_{q \in Q} \sum_{r \in R_q} (\Phi_{q,r}^R Y_{q,r}^R + \Phi_{q,r}^N Y_{q,r}^N) + \sum_{q \in Q} \Phi_q^S Y_q^S \right\} \quad (9a)$$

$$\text{s.t. } X_a^1 \geq Y_{q,r}^R, \quad \forall a \in W_{q,r}, q \in Q, r \in R_q \quad (9b)$$

$$X_k^2 \geq Y_{q,r}^N, \quad \forall k \in K_{q,r}, q \in Q, r \in R_q \quad (9c)$$

$$X_k^3 \geq Y_q^S, \quad \forall k \in N_q, q \in Q \quad (9d)$$

$$Y_q^S \leq \sum_{r \in R_q} (Y_{q,r}^R + Y_{q,r}^N) \leq 1, \quad \forall q \in Q \quad (9e)$$

$$\sum_{a \in W} X_a^1 \leq N^1, \quad (9f)$$

$$\sum_{k \in K} X_k^j \leq N^j, \quad \forall j \in \{2, 3\} \quad (9g)$$

$$X_k^2 + X_k^3 \leq 1, \quad \forall k \in K \quad (9h)$$

$$X_a^1, X_k^2, X_k^3 \in \{0, 1\}, \quad \forall a \in W, k \in K \quad (9i)$$

$$0 \leq Y_{q,r}^R, Y_{q,r}^N, Y_q^S \leq 1 \quad \forall q \in Q, r \in R_q. \quad (9j)$$

TABLE II
NOMENCLATURE OF ST-FCLM

Q, q	the set and index of OD pairs
R_q, r	the set and index of routes that used in traveling between an OD pair q
K, W	the sets of all candidate nodes and links, respectively
$W_{q,r}, a$	the set and index of candidate OWC links on route r between OD pair q where $W_{q,r} \subseteq W$
$K_{q,r}, k$	the set and index of candidate nodes for plug-in charging facilities on route r between OD pair q , where $K_{q,r} \subseteq K$
N_q	the destination node of the OD pair q , where $N_q \subseteq K$
N^j	the given number of OWCs, FCSs, and PLs to be deployed for $j \in \{1, 2, 3\}$, respectively
$Y_{q,r}^R$	=1 if the peak traffic flow between OD pair q on route r is captured, 0 otherwise
$Y_{q,r}^N$	=1 if the non-peak traffic flow between OD pair q on route r is captured, 0 otherwise
Y_q^S	=1 if the PEV static charging demand of OD pair q is captured, 0 otherwise
X_a^1	=1 if an OWC is located at candidate link a , 0 otherwise
X_k^2	=1 if an FCS is located at candidate node k , 0 otherwise
X_k^3	=1 if a PL is located at candidate node k , 0 otherwise

The parameters and variables in this formulation are presented in Table II. The objective function (9a) selects the siting plan $\mathbf{X} = (X_a^1, X_k^2, X_k^3)$ that maximizes the captured cumulative traffic flows via all routes that travelers may choose to travel between each OD pair. The objective function consists of three parts: The first part captures the peak traffic flows by siting the OWCs; The second part captures the non-peak traffic flow by siting the FCSs; The third part captures the PEVs static charging demand by siting the PLs. Constraints (9b) and (9c) ensure that the flow between an OD pair is captured if each link on the route r is traversable after charging in the OWCs or FCSs along the path. These constraints are designed to consider the limited PEV driving range. On route r between OD pairs q , a pre-generated candidate node list $K_{q,r}$ and candidate link list $W_{q,r}$ are used to site the charging facilities to ensure that the route is traversable by the limited

range PEVs. The generation of $K_{q,r}$ and $W_{q,r}$ is discussed in the following paragraph. Constraint (9d) ensures that a PL is sited at the destination node N_q of the OD pair q if the static charging demand of this flow is met. To prevent double-counting, constraint (9e) ensures that charging facilities, either OWCs or FCSs, are sited on one route between each OD pair, which can capture the highest possible flow over the time. Only one type of facilities can capture the covered flow. The highest flows during the peak traffic will be covered by OWCs and then the highest flows during non-peak traffic will be covered by FCSs. Also, this constraint ensures that the PEV static charging demand can only be covered if the flows between OD pairs are covered by either OWCs or FCSs, which ensures that PEVs will be able to reach the PL locations. Constraints (9f) and (9g) ensure that the total number of each type of the deployed charging facilities in the system is less than or equal to a pre-defined number of facilities. Constraint (9h) indicates that only one type of plug-in facilities can be deployed at any system node. Constraint (9i) forces the binary variables to be either 0 or 1. Some binary variables can be relaxed to continuous variables and constraint (9j) specifies their limits. The ST-FCLM is an mixed-integer linear programming (MILP) problem, in which the number of variables and constraints increase exponentially with an increase of OD pairs and number of routes between each q .

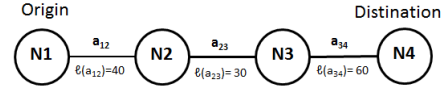


Fig. 1. Example on generation the set of candidate charging facilities sites.

To consider the PEV limited driving range, more than one charging facility may be allocated between an OD pair in the network if the traveling distance between them is longer than the maximum PEV driving range. For each route that travelers may choose between an OD pair, two sets of candidate sites are generated: 1) Set $K_{q,r}$ contains all the candidate nodes for plug-in charging facilities (FCSs or PLs) to ensure that all the links on route r are traversable for a round trip between OD pair q ; 2) Set $W_{q,r}$ contains all candidate links suitable for deploying OWCs. Figure 1 illustrates a simple example of a single OD pair connected through three bidirectional links $\{a_{12}, a_{23}, a_{34}\}$ and four nodes $\{N_1, N_2, N_3, N_4\}$. We define $\ell(\cdot)$ as the length of links. In this example, the PEV range is $\mathcal{R} = 90$. The initial PEV battery SoC is assumed equal to $\frac{\mathcal{R}}{2}$. To complete a round trip without running out of battery charge, the first candidate site for plug-in charging facility is N_2 since PEV can travel through a_{12} with the initial battery SoC. If the length of a_{12} exceeds the initial PEV battery SoC, the first candidate site is N_1 . In both cases, link a_{12} is a candidate for deploying OWC. PEV battery SoC is equal to \mathcal{R} after recharging at a plug-in facility at N_2 or OWC at a_{12} . Then, the PEV can travel through a_{23} and a_{34} . When the PEV reaches N_4 , it must be recharged again in order to return to the origin and complete the round trip via the same route. Hence, another plug-in charging facility should be sited at N_4 or OWC at a_{34} . Therefore, the candidate plug-in charging facility set for

this route is $\{N_2, N_4\}$, and the candidate links for OWC is $\{a_{12}, a_{34}\}$. In order to generalize this approach, Algorithm 1 is used to generate the candidate sites for all OD pairs in a network. All the practical routes being chosen by the travelers should be extracted from the DTA model for this algorithm. In this algorithm, $T(\cdot)$ returns the tail node of a link. The set of links between OD pairs q on route r is denoted by $A_{q,r}$ and link i in this set by $a(i)$, where i is the ordering index.

Algorithm 1 Generating of the candidate site sets

Input: Vehicles range \mathcal{R} , Set of links $A_{q,r}$

Output: Candidate nodes set K , Candidate links set W

```

1:  $K \leftarrow \emptyset, W \leftarrow \emptyset.$ 
2: for each  $q \in Q$  do
3:   for each  $r \in R_q$  do
4:     Set  $i = 1.$ 
5:     Set  $SoC_1 \equiv \frac{\mathcal{R}}{2}$ 
6:     for each  $a(i) \in A_{q,r}$  do
7:       if  $\ell(a(i)) \geq SoC_i$  then
8:          $W_{q,r} \leftarrow W_{q,r} \cup \{a(i)\}$ 
9:          $K_{q,r} \leftarrow K_{q,r} \cup \{T(a(i))\}$ 
10:         $SoC_{i+1} = \mathcal{R} - \ell(a(i))$ 
11:       else
12:          $SoC_{i+1} = SoC_i - \ell(a(i))$ 
13:       end if
14:     end for
15:    $K \leftarrow K \cup K_{q,r}.$ 
16:    $W \leftarrow W \cup W_{q,r}.$ 
17: end for
18: end for

```

IV. SIZING OF CHARGING FACILITIES BASED ON QUEUING THEORY

The ST-FCLM optimizes locations for each type of charging facilities. In this section, queuing theory is used to determine the appropriate capacity for each charging facility (i.e. the number of chargers). The capacity of a charging facility is optimized to satisfy a certain quality of service (QoS) target, mainly the average waiting time of customers to get a charging service during the peak traffic hour. Some assumptions are made in sizing of charging facilities: 1) PEV arrivals at a charging facility follow a Poisson process and the mean arrival rate λ is in proportion to the traffic volumes captured by the facility and the PEV penetration rate. This assumption conforms with the existing vehicle mobility models verified by experiments [33]; 2) The duration of PEV charging using constant charging power is independently and exponentially distributed, with an average duration $1/\mu$. This assumption conforms with the PEV battery charging behavior model [34]; 3) There are C independent and identical chargers at charging facility, and PEVs are served based on a first-come-first-served rule; 4) There are enough waiting spaces at each charging facility. Based on these assumptions, the $M/M/C$ queuing theory [35] is used to model each charging facility in the system.

The mean arrival rate to a charging facility during the rush hour depends on the captured traffic flows, PEV penetration

rate, and the facility type, as follows:

$$\lambda_a^1 = \max \{P \cdot (1 - \sigma) \cdot \beta \cdot f_a(t), \forall t \in T\} \quad \forall a \in \Omega^1 \quad (10a)$$

$$\lambda_k^2 = \max \{P \cdot (1 - \sigma) \cdot (1 - \beta) \cdot f_k(t), \forall t \in T\} \quad \forall k \in \Omega^2 \quad (10b)$$

$$\lambda_d^3 = \max \{P \cdot \sigma \cdot f_d(t), \forall t \in T\} \quad \forall d \in \Omega^3 \quad (10c)$$

where $\lambda_a^1, \lambda_k^2, \lambda_d^3$ represent the mean arrival rate during rush hour to OWC at link a , FCS at node k , and PL at destination node d , respectively. The PEV penetration rate is denoted by P . The percentage of PEV drivers prefer charging in PLs at trip destinations is denoted by σ . The percentage of PEVs capable of charging through wireless power transfer technology in OWCs is denoted by β . The traffic volumes captured by each type of charging facilities are denoted by f_a, f_k, f_d for OWC, FCS, and PL, respectively. The sets of the sited charging facilities are denoted by $\Omega^1, \Omega^2, \Omega^3$ for OWC, FCS, and PL, respectively.

Based on the necessary and sufficient conditions for the stability of the $M/M/C$ queuing model, the minimum number of chargers allocated in a charging facility should satisfy the following inequality [35]:

$$C > \rho = \frac{\lambda}{\mu} \quad (11)$$

where ρ is the traffic intensity. Thereby, the sizing of a charging facility can be formulated as follows:

$$\min_C C \quad (12a)$$

$$s.t. \bar{W} \leq W^{Th} \quad (12b)$$

$$[\rho] < C \leq [C^{max}]. \quad (12c)$$

The objective function in (12a) minimizes the number of chargers required at a charging facility. Constraint (12b) ensures that the expected waiting time \bar{W} of customers at a charging facility is less than or equal the predefined maximum allowable waiting time W^{Th} . The expected waiting time can be calculated as:

$$\bar{W} = \frac{\mathbb{P}(W > 0)}{\mu(C - \rho)} \quad (13a)$$

$$\mathbb{P}(W > 0) = \frac{C \rho^C}{C!(C - \rho)} \quad (13b)$$

$$\sum_{k=0}^{C-1} \frac{\rho^k}{k!} + \frac{C \rho^C}{C!(C - \rho)}$$

where $\mathbb{P}(W > 0)$ is the delay probability or Erlang-C formula. Constraint (12c) ensures that the selected number of chargers is an integer number, indicated by $[\]$, and higher than the traffic intensity to ensure the stability of the system. Additionally, the selected number of chargers should be less than or equal to the maximum number of chargers that can be accommodated by the power distribution network C^{max} [9].

The sizing problem is solved by a search algorithm similar to that in [36]. In this algorithm, the number of chargers is initialized by the integer number, which is higher than the traffic intensity. Then, C is iteratively incremented until all constraints are satisfied. After optimizing the number of chargers, the waiting spaces L at charging facility can be estimated to be higher than or equal to the expected queuing length at the rush hour, as follows

$$L \geq \frac{\rho}{C - \rho} \mathbb{P}(W > 0). \quad (14)$$

In this section, each charging facility is sized in isolation. This model can be extended to a networked charging infrastructure, which can capture the correlation among the charging demands of the nearby charging facilities and then the propagation of congestion [37]. Sizing of a networked charging facilities needs further investigation.

V. NUMERICAL RESULTS

To validate the model and demonstrate its applicability, we select two popular transportation networks, which are known as the Nguyen-Dupuis network [38] and the Sioux Falls network [39]. In each case, four steps are taken: 1) The time-varying traffic flows are simulated based on the road traffic simulator SUMO [40]. The simulation tool iteratively computes the travel times on the network links, then assigns alternative routes to some vehicles on these routes according to the traveling time; 2) The traffic flow dataset is clustered into distinct categories using the GMM algorithm; 3) The set of candidate charging facilities sites is identified based on Algorithm 1; 4) The ST-FCLM is implemented under Python environment with the Gurobi Optimizer 7.5 for 64-bit Windows. The following numerical results are obtained on a laptop computer with a 2.27-GHz Intel(R) Core(TM) i3-M350 CPU and 4 GB of memory.

A. The Nguyen-Dupuis Network

As shown in Figure 2, the Nguyen-Dupuis network contains 13 nodes, 19 links, and 4 OD pairs, which are (1,2), (1,3), (4,2), and (4,3) [38]. Table III lists the daily travel demand between origins and destinations. The hourly distribution of vehicle trips on a weekday as a percentage of daily traffic versus time of day follows the UK national travel survey [41].

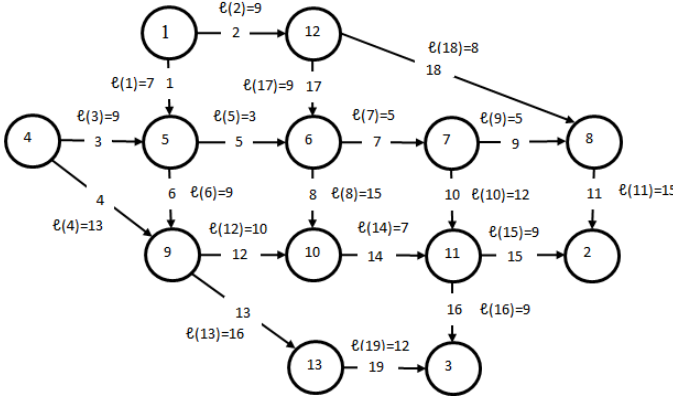


Fig. 2. The Nguyen-Dupuis network.

TABLE III
OD MATRIX OF THE NGUYEN-DUPUIS NETWORK

OD pair	Daily travel demand
(1,2)	11000
(1,3)	24000
(4,2)	13000
(4,3)	6000

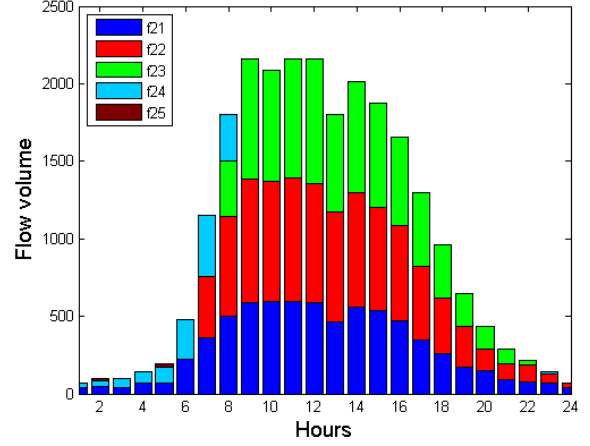


Fig. 3. The Nguyen-Dupuis network traffic flow between OD pair (1,3).

To visualize the traffic simulation output, we plot the time-varying flow volumes between OD pair (1,3) in Figure 3. Table IV lists the traffic flows along with the corresponding traveling routes and route lengths for all OD pairs. The results show that f_{11} between OD pair (1,2) travels through a single route which is the route with the shortest distance. This is because no other flows use the links of this route, permitting the flow to travel without congestion. However, drivers use multiple routes in traveling between all other OD pairs in the network since the links of these routes are shared among multiple flows. Therefore, these links are congested, so travelers choose the routes with minimum traveling time between their OD pairs rather than the routes with the shortest distance. Table IV also shows the cumulative traffic flows (after unity-based normalization) during the peak Φ^R and non-peak Φ^N traffic periods, in addition to the static PEV charging demand Φ^S at the destination nodes. The sets of candidate charging facility sites K, W are determined based on Algorithm 1, with assuming that the PEV range is $\mathcal{R} = 24$, which is longer than the longest link in the network.

In formulating the ST-FCLM, the limits on the numbers of OWCs, FCSs, and PLs are set to be less than or equal 3,4,1, respectively. As shown in Figure 4, the solution locates OWCs on links $\{4, 14, 17\}$ to cover flows $\{f_{22}, f_{32}\}$, which represent 32.23% of the overall traffic flows in the network. The FCSs are deployed at nodes $\{4, 9, 12, 13\}$ to cover flows $\{f_{11}, f_{42}\}$, which represent 28.32% of the overall traffic flows in the network. Note that f_{22}, f_{32} and f_{42} are not through the shortest distance routes between the OD pairs, but the routes with the highest traffic volumes. A PL is deployed at node $\{2\}$ to cover 55.56% of the overall static charging demand. The percentage of overall *en route* charging demand covered by the charging facilities is 60.55%. This percentage is the maximum traffic flows can be covered in this network, because only one route between each OD pair can be covered to prevent double counting of the flows. A higher percentage of traffic flows can be covered if constraint (9e) is relaxed.

The parameter setting for sizing of charging facilities is as follows. Currently popular PEV models (e.g., Nissan LEAF

TABLE IV
FLOWS ROUTES AND CANDIDATE SITES SETS FOR THE NGUYEN-DUPUIS NETWORK AT $\mathcal{R} = 24$

OD pair	Flow denotation	Route by links	Route length	Φ^R	Φ^N	Φ^S	K	W
(1,2)	f_{11}	2-18-11	32	1.000	1.000	20.37%	12	18
(1,3)	f_{21}	1-5-7-10-16	36	0.603	0.714	44.44%	6, 11	7, 16
	f_{22}	2-17-8-14-16	49	0.803	0.669		12, 10	17, 14
	f_{23}	2-17-7-10-16	44	0.740	0.451		12, 7	17, 10
	f_{24}	1-6-13-19	44	0.036	0.334		5, 9, 13	6, 13, 19
	f_{25}	1-5-8-14-16	41	0.000	0.012		6, 11	8, 16
(4,2)	f_{31}	3-5-7-9-11	37	0.340	0.443	24.07%	5, 8	5, 11
	f_{32}	4-12-14-15	39	0.842	0.738		4, 10	4, 14
(4,3)	f_{41}	3-5-7-10-16	38	0.143	0.189	11.11%	5, 11	5, 16
	f_{42}	4-13-19	41	0.402	0.356		4, 9, 13	4, 13, 19

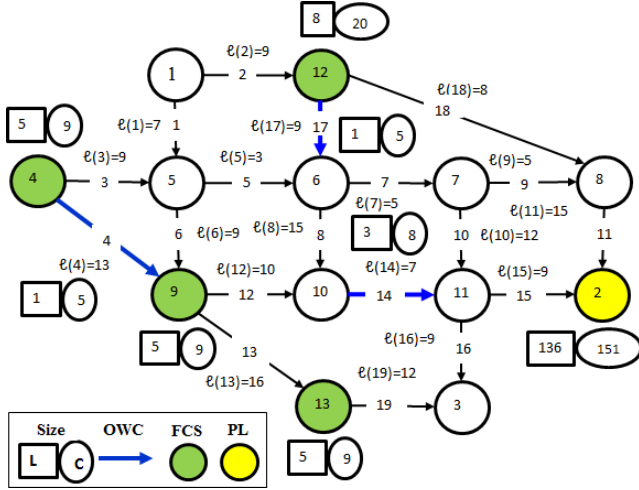


Fig. 4. ST-FCLM solution for the Nguyen-Dupuis network.

2018) have battery capacity 40 kWh. Such PEV can be fully charged using AC level 2 charger (7.4 kW) in 6 hours and DC fast charger (50 kW) in 45 minutes [42]. It is recommended to charge PEV to about 80% SoC to reduce time during charging [29]. Thus, the mean charging time is set to 3 hours ($\mu = 0.3$) in PLs and 20 minutes ($\mu = 3$) in FCSs. Although the standard of charging power for OWC has not been finalized yet, it is assumed that the mean charging time with 22 kW is 10 minutes ($\mu = 6$) [5]. The maximum waiting times at OWC, FCS, and PL are set to 5, 15, and 60 minutes, respectively. The penetration rate of PEVs in the system is $P = 20\%$. The percentage of users prefer to charge their PEVs in PLs is set to $\sigma = 60\%$. The percentage of PEVs capable of charging through OWC is set to $\beta = 30\%$. Figure 4 shows the number of chargers C and waiting space L at charging facilities.

Substantial differences appear when comparing the results of ST-FCLM with those of arc-cover path-cover flow refueling location model (AC-PC FRLM) proposed in [13] for the same network. There are two main differences between ST-FCLM and AC-PC FCLM: 1) In the AC-PC FRLM, drivers are assumed traveling through the shortest distance routes between OD pairs. Then, the siting model is restricted to cover the charging demand on those routes. On the other hand, in the ST-FCLM, drivers are assumed traveling through the routes with minimum travel times to their destinations. Thereby, the ST-FCLM considers all the feasible routes that travelers may

choose for each OD pair to minimize their travel time. Both the spatial and temporal distributions of traffic flows are then used in siting of charging facilities in locations that maximize the covered traffic flows; 2) The AC-PC FRLM locates a single type of charging facilities on the transportation network nodes. On the other hand, the ST-FCLM utilizes the clustered traffic flow dataset in siting multiple types of charging facilities.

To compare the ST-FCLM and AC-PC FCLM, we analyze the effect of varying the number of sited facilities on the percentages of covered traffic flows. As shown in Figure 5, the ST-FCLM covers either higher or as same traffic flows as AC-PC FRLM. As shown in Figure 5, the AC-PC FRLM covers only 12.88% of the overall flows in the network with two charging facilities, although it covers 20.37% with one facility. This is because, with two charging facilities, this model covers flow f_{21} that has more traveling demand than flow f_{11} , which can be covered by one facility. However, the travelers between OD pair (1,3) choose various distance routes during their trips and are not restricted to the shortest distance route. On the other hand, the ST-FCLM always covers the routes with the highest traffic volumes. Moreover, the ST-FCLM can cover up to 60.55% by deploying five charging facilities. However, the maximum traffic flows can be covered in the AC-PC FRLM is 43.9%. Consequently, the ST-FCLM outperforms the flow covering model, where traveler route choices are only governed by the distance of routes.

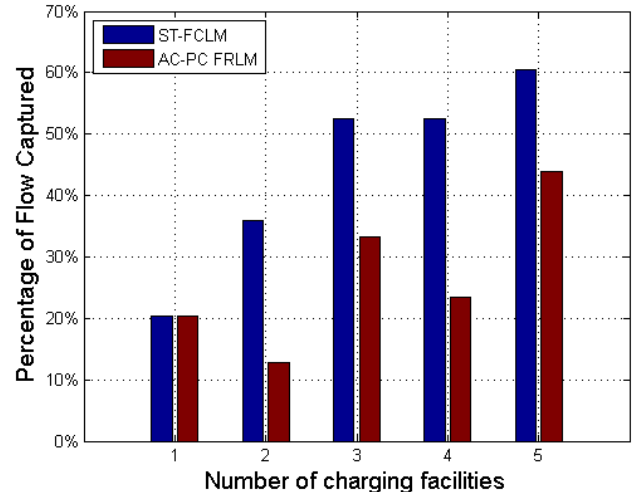


Fig. 5. Comparison between ST-FCLM and AC-PC FRLM when $\mathcal{R} = 24$.

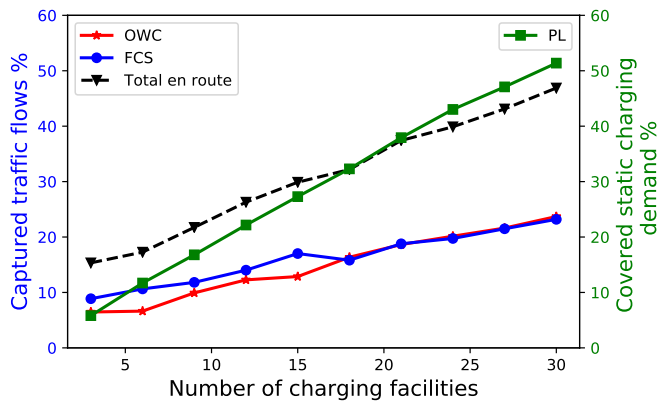


Fig. 6. Implementing the ST-FCLM on the Sioux Falls network.

B. The Sioux Falls Network

To validate our model on a larger network, with more realistic topology and demand properties, we select the well-known transportation network of Sioux Falls, South Dakota, USA. The Sioux Falls network consists of 24 nodes, 76 links, and 576 OD pairs [39]. The topology of the Sioux Falls network in addition to other network attributes, such as OD matrix and link capacity, are reported in [39]. All nodes are candidate sites for FCSs and PLs, and all links are candidate sites for OWCs.

The DTA simulation for the Sioux Falls network converges to the Wardrops user equilibrium after three iterations. The number of generated flow vectors between the 576 OD pairs is 1656. Each flow vector has a specific traveling route between the corresponding OD pair. The flow vectors contain the discretized values of traffic volumes on the corresponding traveling routes for 24-time slots over a typical weekday. The traffic flow dataset is partitioned into two categories based on the GMM clustering algorithm. The number of Gaussian components is chosen to be two components, which minimize the BIC score. Table V lists the GMM parameters for the two Gaussian components. The EM algorithm reaches convergence after three iterations.

TABLE V
GMM COMPONENT PARAMETERS

i	ω_i	μ_i	Σ_i
1	0.43750854	1.88507101	3.9677486
2	0.56249146	14.59745472	15.14277279

We implement the ST-FCLM on the Sioux Falls network, with the REV range $\mathcal{R} = 100$ km. Figure 6 shows the captured traffic flows and the covered static charging demand as a function of the number of charging facilities. The number of deployed facilities is increased gradually until 10 facilities from each type are deployed. It is observed that around 47% and 51% of the *en route* and *static* PEV charging demand, respectively, can be covered by the 10 facilities from each type.

VI. CONCLUSION AND FUTURE WORK

In this paper, we propose the spatial-temporal flow capturing location model. This model locates three types of charging facilities based on the spatial-temporal distribution of the traffic flows. A simulation-based DTA model is used to estimate the time-varying traffic flows between all OD pairs in the network. Then, the traffic flow dataset is clustered by the GMM algorithm according to the temporal characteristics to identify the time periods in which the traffic flows are high or low. Our model captures the traffic flows during peak and non-peak traffic periods by OWCs and FCSs, respectively. The ST-FCLM deploys PLs at the destination nodes of the trips to cover the static PEV charging demand. Thus, our model makes use of different characteristics and usage patterns of each charging technology. The simulation results based on the Nguyen-Dupuis and Sioux Falls networks show that the proposed model captures a higher percentage of traffic flows with the same number of facilities when compared with an existing model based only on spatial characteristics of the traffic flows. Additionally, our model can be implemented on a relatively large transportation network with a comparatively high number of OD pairs.

Our model can be extended by optimizing the number of charging facilities of various types to maximize user satisfaction within a budget limit. This extension would address the trade-off between establishing expensive user preferred charging facilities and deploying more inexpensive facilities to maximize the captured traffic flow. More research is required to derive a user satisfaction index. Then, develop a siting model that counterbalance the percentage of covered charging demand and user satisfaction.

ACKNOWLEDGMENT

The authors would like to thank the anonymous reviewers whose constructive comments helped improving the quality of this paper in both technical contents and presentation. This work was supported by a research grant from the Natural Sciences and Engineering Research Council (NSERC) of Canada.

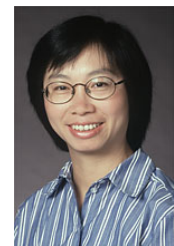
REFERENCES

- [1] The International Energy Agency (IEA), “Global EV outlook 2017, two million and counting,” 2017.
- [2] A. Abdalrahman and W. Zhuang, “A survey on PEV charging infrastructure: Impact assessment and planning,” *Energies*, vol. 10, no. 10, p. 1650, 2017.
- [3] C.-H. Ou, H. Liang, and W. Zhuang, “Investigating wireless charging and mobility of electric vehicles on electricity market,” *IEEE Trans. Ind. Electron.*, vol. 62, no. 5, pp. 3123–3133, 2015.
- [4] Z. Bi, T. Kan, C. C. Mi, Y. Zhang, Z. Zhao, and G. A. Keoleian, “A review of wireless power transfer for electric vehicles: Prospects to enhance sustainable mobility,” *Appl. Energ.*, vol. 179, pp. 413–425, 2016.
- [5] S. Y. Choi, S. Y. Jeong, B. W. Gu, G. C. Lim, and C. T. Rim, “Ultraslim s-type power supply rails for roadway-powered electric vehicles,” *IEEE Trans. Power Electron.*, vol. 30, no. 11, pp. 6456–6468, 2015.
- [6] G. Wang, Z. Xu, F. Wen, and K. P. Wong, “Traffic-constrained multiobjective planning of electric-vehicle charging stations,” *IEEE Trans. Power Del.*, vol. 28, no. 4, pp. 2363–2372, 2013.
- [7] A. Lam, Y.-W. Leung, and X. Chu, “Electric vehicle charging station placement: Formulation, complexity, and solutions,” *IEEE Trans. Smart Grid*, vol. 5, no. 6, pp. 2846–2856, 2014.

- [8] W. Tu, Q. Li, Z. Fang, S.-I. Shaw, B. Zhou, and X. Chang, "Optimizing the locations of electric taxi charging stations: A spatial-temporal demand coverage approach," *Transport. Res. C-Emer.*, vol. 65, pp. 172–189, 2016.
- [9] Y. Xiang, J. Liu, R. Li, F. Li, C. Gu, and S. Tang, "Economic planning of electric vehicle charging stations considering traffic constraints and load profile templates," *Appl. Energ.*, vol. 178, pp. 647–659, 2016.
- [10] M. Kuby and S. Lim, "The flow-refueling location problem for alternative-fuel vehicles," *Socioecon. Plann. Sci.*, vol. 39, no. 2, pp. 125–145, 2005.
- [11] J. Ko, T.-H. T. Gim, and R. Guensler, "Locating refuelling stations for alternative fuel vehicles: a review on models and applications," *Transport Rev.*, vol. 37, no. 5, pp. 551–570, 2017.
- [12] M. J. Hodgson, "A flow-capturing location-allocation model," *Geogr. Anal.*, vol. 22, no. 3, pp. 270–279, 1990.
- [13] I. Capar, M. Kuby, V. J. Leon, and Y.-J. Tsai, "An arc cover–path-cover formulation and strategic analysis of alternative-fuel station locations," *Eur. J. Oper. Res.*, vol. 227, no. 1, pp. 142–151, 2013.
- [14] Y. Huang, S. Li, and Z. S. Qian, "Optimal deployment of alternative fueling stations on transportation networks considering deviation paths," *Netw. Spat. Econ.*, vol. 15, no. 1, pp. 183–204, 2015.
- [15] B. Yildiz, O. Arslan, and O. E. Karaşan, "A branch and price approach for routing and refueling station location model," *Eur. J. Oper. Res.*, vol. 248, no. 3, pp. 815–826, 2016.
- [16] F. Wu and R. Sioshansi, "A stochastic flow-capturing model to optimize the location of fast-charging stations with uncertain electric vehicle flows," *Transp. Res. D Transp. Environ.*, vol. 53, pp. 354–376, 2017.
- [17] R. Riemann, D. Z. Wang, and F. Busch, "Optimal location of wireless charging facilities for electric vehicles: flow-capturing location model with stochastic user equilibrium," *Transport. Res. C-Emer.*, vol. 58, pp. 1–12, 2015.
- [18] Y.-W. Wang and C.-C. Lin, "Locating multiple types of recharging stations for battery-powered electric vehicle transport," *Transport. Res. E-Log.*, vol. 58, pp. 76–87, 2013.
- [19] Z. Chen, W. Liu, and Y. Yin, "Deployment of stationary and dynamic charging infrastructure for electric vehicles along traffic corridors," *Transport. Res. C-Emer.*, vol. 77, pp. 185–206, 2017.
- [20] C. Luo, Y.-F. Huang, and V. Gupta, "Placement of EV charging stations balancing benefits among multiple entities," *IEEE Trans. Smart Grid*, vol. 8, no. 2, pp. 759–768, 2017.
- [21] C. J. Sheppard, A. Harris, and A. R. Gopal, "Cost-effective siting of electric vehicle charging infrastructure with agent-based modeling," *IEEE Trans. Transport. Electric.*, vol. 2, no. 2, pp. 174–189, 2016.
- [22] H. Zhang, Z. Hu, Z. Xu, and Y. Song, "An integrated planning framework for different types of PEV charging facilities in urban area," *IEEE Trans. Smart Grid*, vol. 7, no. 5, pp. 2273–2284, 2016.
- [23] Y.-C. Chiu, J. Bottom, M. Mahut, A. Paz, R. Balakrishna, T. Waller, and J. Hicks, "Dynamic traffic assignment: A primer," *Transportation Research E-Circular*, no. E-C153, 2011.
- [24] C. Gawron, "Simulation-based traffic assignment: Computing user equilibria in large street networks," Ph.D. dissertation, 1999.
- [25] P. Kachroo and N. Shlayan, "Dynamic traffic assignment: A survey of mathematical models and techniques," in *Advances in Dynamic Network Modeling in Complex Transportation Systems*. Springer, 2013, pp. 1–25.
- [26] D. Boyce, D.-H. Lee, and B. Ran, "Analytical models of the dynamic traffic assignment problem," *Netw. Spat. Econ.*, vol. 1, no. 3, pp. 377–390, 2001.
- [27] F. Calabrese, G. Di Lorenzo, L. Liu, and C. Ratti, "Estimating origin-destination flows using opportunistically collected mobile phone location data from one million users in boston metropolitan area," *IEEE Pervasive Computing*, vol. 10, no. 4, pp. 36–44, 2011.
- [28] S. Rasouli and H. Timmermans, "Uncertainty in travel demand forecasting models: literature review and research agenda," *Transportation letters*, vol. 4, no. 1, pp. 55–73, 2012.
- [29] H. Zhang, S. J. Moura, Z. Hu, and Y. Song, "PEV fast-charging station siting and sizing on coupled transportation and power networks," *IEEE Trans. Smart Grid*, vol. 9, no. 4, pp. 2595–2605, 2018.
- [30] B. Selim, O. Alhussein, S. Muhaidat, G. K. Karagiannidis, and J. Liang, "Modeling and analysis of wireless channels via the mixture of Gaussian distribution," *IEEE Trans. Veh. Technol.*, vol. 65, no. 10, pp. 8309–8321, 2016.
- [31] D. Reynolds, "Gaussian mixture models," *Encyclopedia of biometrics*, pp. 827–832, 2015.
- [32] P. D. McNicholas, *Mixture model-based classification*. CRC Press, 2016.
- [33] N. Wisitpongphan, F. Bai, P. Mudalige, V. Sadekar, and O. Tonguz, "Routing in sparse vehicular Ad Hoc wireless networks," *IEEE J. Sel. Areas Commun.*, vol. 25, no. 8, pp. 1538–1556, 2007.
- [34] O. Hafez and K. Bhattacharya, "Queuing analysis based PEV load modeling considering battery charging behavior and their impact on distribution system operation," *IEEE Trans. Smart Grid*, vol. 9, no. 1, pp. 261–273, 2018.
- [35] J. Sztrik, "Basic queueing theory," *University of Debrecen, Faculty of Informatics*, vol. 193, 2012.
- [36] M. Ismail, I. S. Bayram, M. Abdallah, E. Serpedin, and K. Qaraqe, "Optimal planning of fast PEV charging facilities," in *IEEE First Workshop on Smart Grid and Renewable Energy (SGRE)*, 2015, pp. 1–6.
- [37] H. Liang, I. Sharma, W. Zhuang, and K. Bhattacharya, "Plug-in electric vehicle charging demand estimation based on queueing network analysis," in *Proc. IEEE PES Gen. Meet.*, Jul. 2014, pp. 1–5.
- [38] S. Nguyen and C. Dupuis, "An efficient method for computing traffic equilibria in networks with asymmetric transportation costs," *Transport. Sci.*, vol. 18, no. 2, pp. 185–202, 1984.
- [39] Transportation Networks for Research Core Team. Transportation Networks for Research., "Sioux falls transportation network," <https://github.com/bstabler/TransportationNetworks>, accessed: May 12, 2018.
- [40] D. Krajzewicz, J. Erdmann, M. Behrisch, and L. Bieker, "Recent development and applications of SUMO - Simulation of Urban MObility," *International Journal On Advances in Systems and Measurements*, vol. 5, no. 3&4, pp. 128–138, December 2012.
- [41] UK National Travel Survey: 2010, "When people travel," <https://www.gov.uk/government/statistics/national-travel-survey-2010>, accessed: Jan 5, 2018.
- [42] Nissan LEAF 2018, "Charging specifications," <https://www.evbox.com/electric-cars/nissan/nissan-leaf>, accessed: Oct 12, 2018.



Ahmed Abdalrahman received the BSc. degree (First Class Hons.) from Thebes Higher Institute of Engineering, Egypt, in 2008; and the MSc. degree from Ain Shams University, Egypt, in 2013, all in Electrical Engineering. He is a research assistant and currently working towards his Ph.D. degree at the Department of Electrical and Computer Engineering, University of Waterloo, Canada. His current research interests include smart grids, electric vehicles, and charging station planning.



Weihua Zhuang (M93-SM01-F08) has been with the Department of Electrical and Computer Engineering, University of Waterloo, Canada, since 1993, where she is a Professor and a Tier I Canada Research Chair in Wireless Communication Networks. She is the recipient of 2017 Technical Recognition Award from IEEE Communications Society Ad Hoc & Sensor Networks Technical Committee, and a co-recipient of several best paper awards from IEEE conferences. Dr. Zhuang was the Editor-in-Chief of IEEE Transactions on Vehicular Technology (2007–2013), Technical Program Chair/Co-Chair of IEEE VTC Fall 2017 and Fall 2016, and the Technical Program Symposia Chair of the IEEE Globecom 2011. She is a Fellow of the IEEE, the Royal Society of Canada, the Canadian Academy of Engineering, and the Engineering Institute of Canada. Dr. Zhuang is an elected member in the Board of Governors and VP Publications of the IEEE Vehicular Technology Society. She was an IEEE Communications Society Distinguished Lecturer (2008–2011).